Precise determination of the κ resonance from a dispersive πK analysis

PWA 12/ATHOS 7

September 9, 2021

WILLIAM & MARY

CHARTERED 1693

Jefferson Lab

Exploring the Nature of Matter

Arkaitz Rodas

Table of Contents

1 Introduction
1.1 Motivation
1.2 First principles

2 Results
2.1 πK dispersive analysis
2.2 Spectroscopy and dispersion relations

3 Summary

Motivation: κ

- Debated for decades
- "We are beginning to think that κ should be classified along with flying saucers, the Loch Ness Monster, and the Abominable Snowman" (Data on Particles and Resonant States,1967)
- "Confirmed soon" Anonymous PDG member 2021

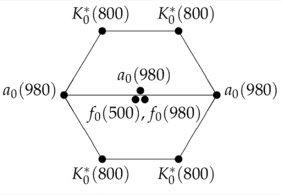

- One of the broadest resonances
- Cannot be interpreted as pure $q\bar{q}$
- Vicinity of the πK $S^{1/2}$ threshold

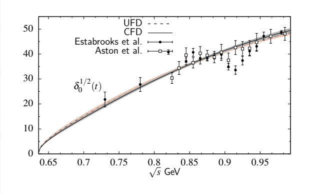

Motivation

- Most of its determinations → simple models
- Scalar nonet, and $\kappa \sim \sigma$

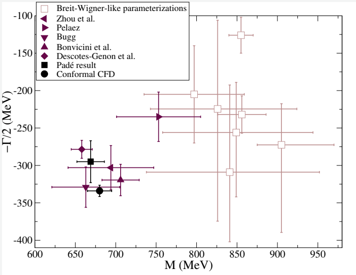

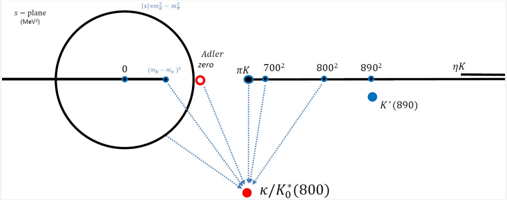

- Too broad to be determined using simple models
- Threshold behavior (ChPT), Adler Zero and LHC play a role
- Same problems in Lattice QCD at low m_π mass

Motivation: πK

- πK scattering $\rightarrow$ final state in hadronic strange processes
- Heavy decays, CP violation, τ decays JHEP 09 031, JHEP 09 042, PLB 804 135371
- $\pi\pi \rightarrow K\bar{K} \Rightarrow$ new physics, g-2...

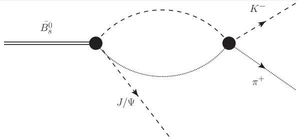

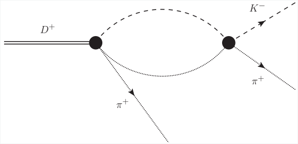

- π, K pseudo-Goldstone Bosons $\rightarrow$ ChPT $\rightarrow$ Scattering Lengths
- UChPT $\rightarrow$ Good description, not suited for high precision

  Nucl.Phys.B 587 331-362, Phys.Rev.D 65 054009
- Experimental groups need robust params $\rightarrow$ LHCb for CP
- New experiment $\rightarrow$ KLF

πK scattering lengths

- Tension between Lattice and ChPT calculations
- SU(3) ChPT does not seem to be converging well

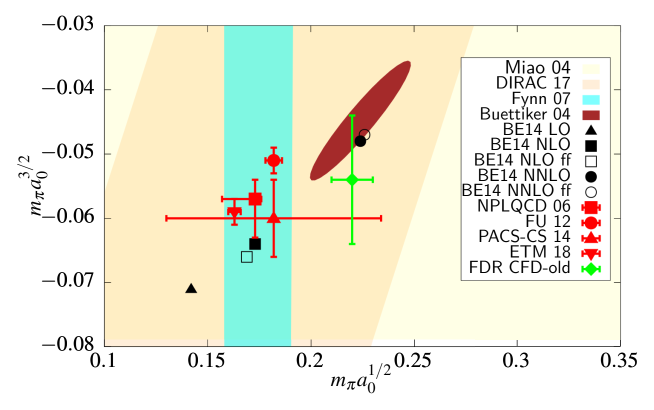

- For all these reasons ⇔ Dispersion Relations

Motivation

- Experiment cannot access πK directly

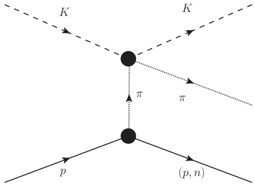

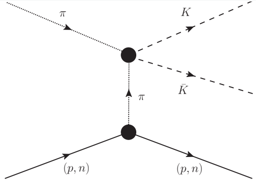

- No precise data at threshold
- Big systematic uncertainties

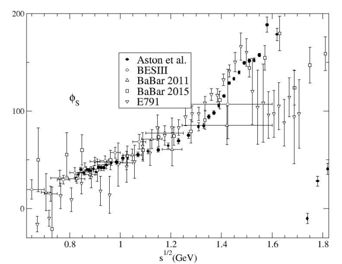

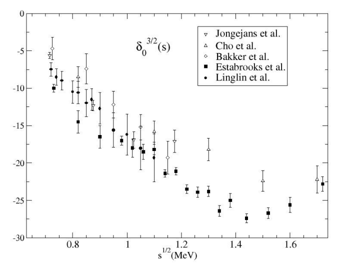

Table of Contents

1 Introduction

1.1 Motivation

1.2 First principles

2 Results

2.1 πK dispersive analysis

2.2 Spectroscopy and dispersion relations

3 Summary

S-matrix principles: Unitarity

- UNITARITY $\Leftrightarrow$ probability $\sum |\langle f|S|i\rangle|^2 = 1$
- Both right and left branch cuts $SS^\dagger = I \Rightarrow F - F^\dagger = \mathrm{i}FF^\dagger$.
- Elastic unitarity $\rightarrow S^{II}(z) = \frac{1}{S^I(z)}$
- Zero of $S^I(z) \rightarrow$ pole of $S^{II}(z)$

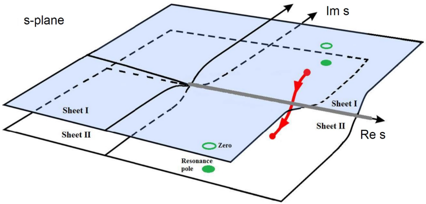

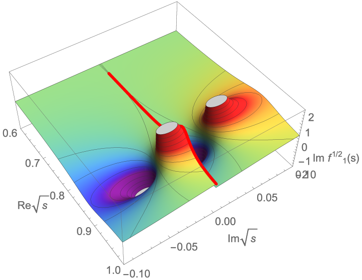

S-matrix principles: Analiticity and Crossing

- CAUSALITY⇔ANALITICITY

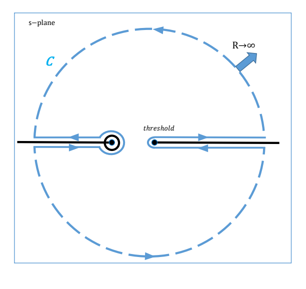

- No poles in the first sheet

$$F(s,t) = \frac{1}{\pi}\int_{s_{th}}^{\infty} ds' \frac{\operatorname{Im} F(s',t)}{s'-s} + LHC$$

- Structures → unitarity, bound states,cusp

- Together with CROSSING → Mandelstam analyticity

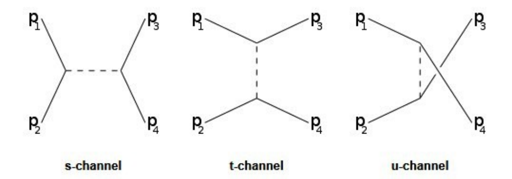

Table of Contents

1 Introduction

1.1 Motivation

1.2 First principles

2 Results

2.1 πK dispersive analysis

2.2 Spectroscopy and dispersion relations

3 Summary

Amplitudes

- Two independent amplitudes I=1/2, 3/2.
- s-channel πK and t-channel $\pi\pi \to K\bar{K}$

$$F^+(s,t) = \frac{1}{3}F^{1/2}(s,t) + \frac{2}{3}F^{3/2}(s,t) = \frac{G^{I_t=0}(t,s)}{\sqrt{6}},$$

$$F^-(s,t) = \frac{1}{3}F^{1/2}(s,t) - \frac{1}{3}F^{3/2}(s,t) = \frac{G^{I_t=1}(t,s)}{2}.$$

- Symmetric and antisymmetric amplitudes under $s \leftrightarrow u$ exchange
- Customary decomposition in partial waves

$$F^I(s,t) = 16\pi \sum_\ell (2\ell+1) f_\ell^I(s) P(z_s(t)),$$

$$G^I(t,s) = 16\pi\sqrt{2} \sum_\ell (2\ell+1)(q_\pi q_K)^\ell g_\ell^I(t) P(z_t(s)).$$

Forward dispersion relations

Phys.Rev. D93 074025

- Combining the First Principles
- Example, amplitude DR, $t=0$

$$\mathrm{Re}\,F^I(s) = F^I(s_{th}) + \frac{(s-s_{th})}{\pi}$$

$$PV\int_{s_{th}}^{\infty} ds' \left[\frac{\mathrm{Im}\,F^I(s')}{(s'-s)(s'-s_{th})} + (-1)^I \frac{\mathrm{Im}\,F^I(s')}{(s'+s-2\Sigma_{\pi K})(s'+s_{th}-2\Sigma_{\pi K})}\right],$$

- If we project $F^I(s) \to f_\ell^I(s)$
  1. We need Input $\to F^I(s), f_\ell^I(s)$
  2. We get DR

- We recover $\mathrm{Re}\,F^I(s)$
  1. Stringent constrains
  2. Perform stable analytic continuation

UFD Input:Elastic region

Phys.Rev. D93 074025

- Unitarity for partial waves

$$f_l^I(s) = \frac{1}{\sigma(s)} \frac{1}{cot\,\delta_l^I(s) - i},$$

- with $cot\,\delta_l^I(s) = \frac{\sqrt{s}}{2q^{2l+1}} \sum B_n \omega(s)^n \rightarrow$ conformal map
- Inelastic region $\rightarrow$ pheno fits
- 8 πK PW $\sim$ 1.8 GeV
- 5 $\pi\pi \rightarrow K\bar{K}$ PW $\sim$ 2 GeV

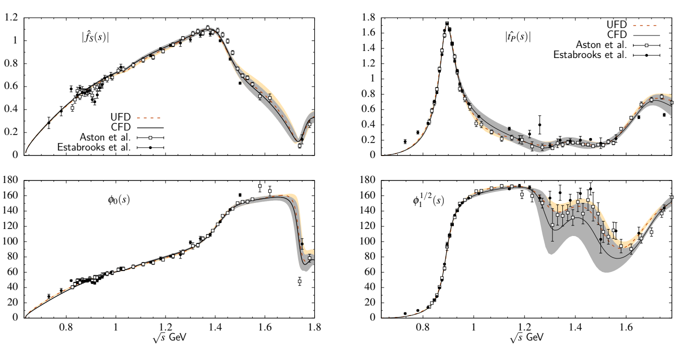

Forward Dispersion relations Phys.Rev. D93 074025

- Amplitudes built using the whole tower of partial waves
- Two independent amplitudes F^+ and F^-
- We define a penalty function $\hat{d}^2 = \frac{1}{N}\sum_i^N \left(\frac{Re(F^I_{out} - F^I_{fit})(s_i)}{\Delta Re\,(F^I_{out} - F^I_{fit})(s_i)} \right)^2$
- Above 1.8 GeV discrepancies too big

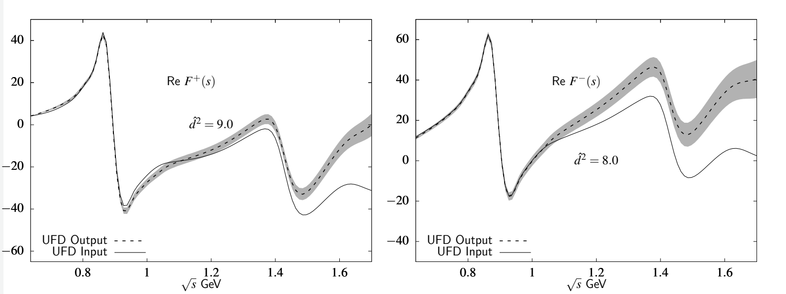

- Room for improvement → Constrained fits

Forward Dispersion relations

Phys.Rev. D93 074025

- Amplitudes built using the whole tower of partial waves
- Two independent amplitudes F^+ and F^-
- We define a penalty function $\hat{d}^2 = \frac{1}{N}\sum_i^N \left(\frac{Re(F^I_{out} - F^I_{fit})(s_i)}{\Delta Re(F^I_{out} - F^I_{fit})(s_i)} \right)^2$
- Above 1.8 GeV discrepancies too big

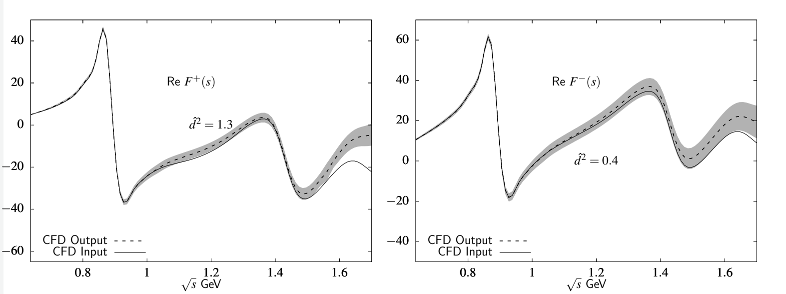

- Very good agreement

DR for πK and $\pi\pi \to K\bar{K}$ 2010.11222, Invited Phys.Rep.

1. We build *DR*
2. Define Penalty function $\hat{d}^2_{DR} = \frac{1}{N}\sum_i^N \left(\frac{Re(f_{out}-f_{fit})(s_i)}{\Delta Re(f_{out}-f_{fit})(s_i)}\right)^2$
3. We minimize a global $\chi^2 = W_1\chi^2_{data} + W_2\hat{d}^2{}_{DR}$
4. Weights $(W_i)\sim$ d.o.f

✔ Forward Dispersion Relations

Phys.Rev.D 93 074025

1. Very simple
2. Applicable to arbitrary high energies

✔ PWDR for πK and $\pi\pi \to K\bar{K}$

2010.11222, Eur.Phys.J.C 78 897

1. Fixed-t DR for πK only
2. Hyperbolic dispersion relations for both
3. Omnès-Muskhelishvili problem
4. Aplicable $\sim \mathbb{O}(1)$ GeV

HDR/Fixed$-t$ both πK and $\pi\pi \to K\bar{K}$ 2010.11222, Invited to Phys.Rep.

- Fixed-t only used for $\pi K \to \pi K$ inputs dominate
- HDR used for both πK and $\pi\pi \to K\bar{K}$ channels
- $(s-a_i)(u-a_i) = b$ with a_s, a_t used to maximize to applicability region

$$f_0^+(s) = a_0^+ + \frac{1}{\pi}\sum_l \left(\int_{s_{th}}^{\infty} ds' K_{0l}^+(s,s') Im f_l^+(s') + \int_{4m_\pi^2}^{\infty} dt' G_{02l}^+(s,t') Im g_{2l}^0(t') \right)$$

$$g_0^0(t) = \frac{\sqrt{3}}{2} m_+ a_0^+ + \frac{1}{\pi}\sum_l \left(\int_{m_+^2}^{\infty} ds' G_{0,l}^+(t,s') Im f_l^+(s') + t \int_{4m_\pi^2}^{\infty} \frac{dt'}{t'} G_{0,2l}^0(t,t') Im g_{2l}^0(t') \right)$$

- Both channels are coupled

πK UFD 2010.11222, Invited to Phys.Rep.

- Some of the dispersion relations are severely deviated
- The scattering lengths are not compatible with the DR

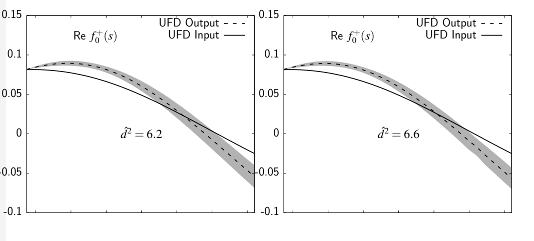

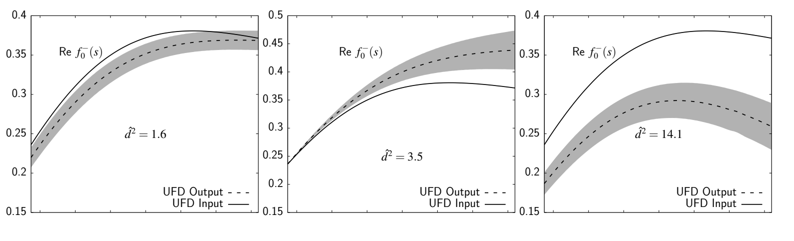

πK CFD 2010.11222, Invited to Phys.Rep.

- Remarkable agreement
- All DR now compatible from threshold on

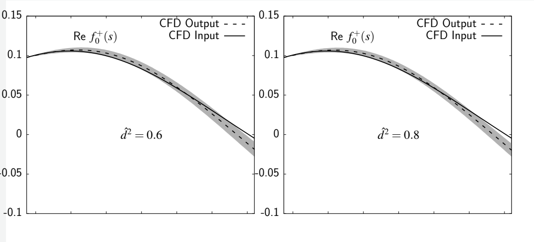

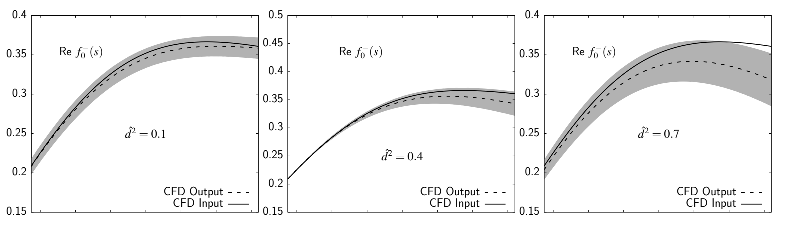

- Average $\hat{d}^2/DR \simeq 5.5\,(\text{UFD}) \rightarrow 0.6\,(\text{CFD})$
- 13 partial waves $\rightarrow \chi^2/dof \simeq 1\,(\text{UFD}) \rightarrow 1.6\,(\text{CFD})$

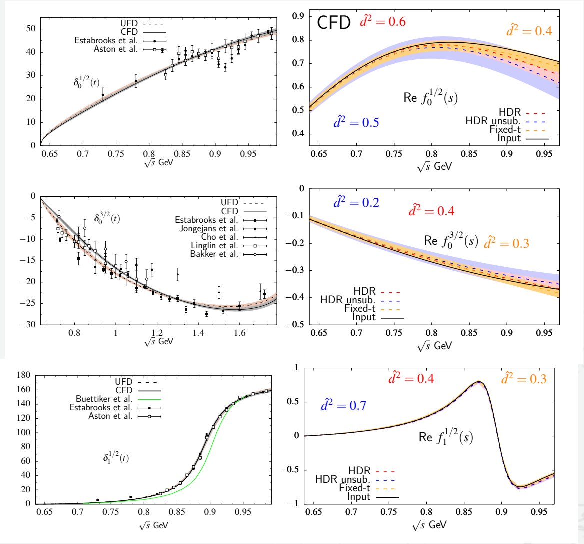

- CFD result for scattering lengths:

	UFD	CFD	Paris group
$a_0^{1/2}$	0.241±0.013	0.224±0.011	0.224±0.022
$a_0^{3/2}$	-0.067±0.014	-0.048±0.006	-0.0448± 0.0077

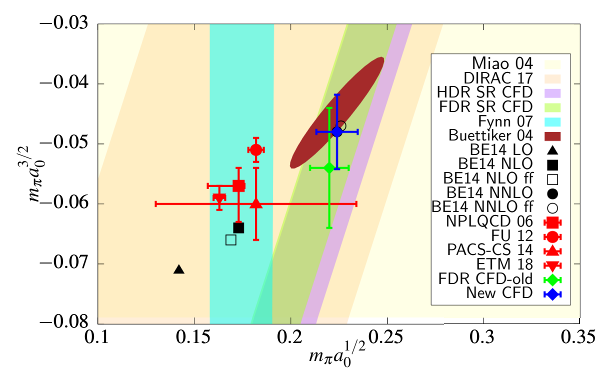

Reminder: Unitarity

- UNITARITY $\Leftrightarrow$ probability $\sum |\langle f|S|i\rangle|^2 = 1$
- Elastic unitarity $\rightarrow S^{II}(z) = \frac{1}{S^{I}(z)}$
- Zero of $S^{I}(z) \rightarrow$ pole of $S^{II}(z)$

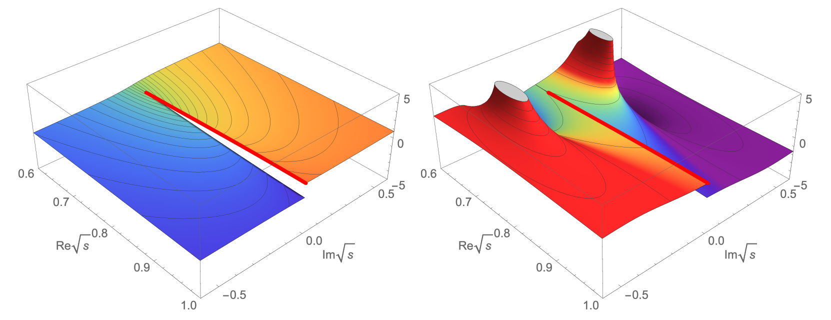

CFD $K_0^*(700)/\kappa$ pole

Phys.Rev.Lett. 172001

- Stable result AFTER constraining
- All uncertainties have been taken into account

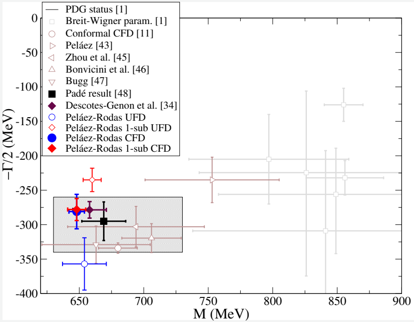

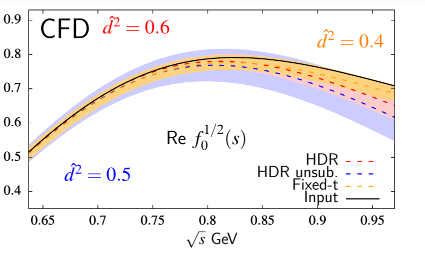

$$\sqrt{s_p} = (648 \pm 7) - i(560 \pm 32)/2 \text{ MeV} \quad \text{HDR}$$

$$\sqrt{s_p} = (658 \pm 13) - i(557 \pm 24)/2 \text{ MeV} \quad \text{Descotes-Genon,Moussallam}$$

$$\sqrt{s_p} = (680 \pm 50) - i(600 \pm 80)/2 \text{ MeV} \quad \text{PDG}$$

Table of Contents

1 Introduction
1.1 Motivation
1.2 First principles

2 Results
2.1 πK dispersive analysis
2.2 Spectroscopy and dispersion relations

3 Summary

πK dispersive analysis: Summary

- DR analysis on almost all πK available data
  1. Pruning on the data
  2. Result $\rightarrow$ simple params compatible with both Data and DR
  3. Model independent determination of the scattering lengths
- DR applied to spectroscopy
  1. Extraction of the $\kappa/K_0^*(700)$ with 2 DR $\rightarrow$ exists
  2. Extraction of the $K^*(892)$ using 3 DR

Spare slides!

πK scattering lengths

$$F^I(s_{th},0) = 8\pi m_+ a_0^I,$$

where $m_+ = m_\pi + m_K$

- At LO

$$a_0^- \propto \frac{1}{f_\pi^2} \qquad a_0^+ = \mathcal{O}(m_+^4).$$

- NLO $\longrightarrow$ LECs L_{1-8}

$$a_0^- \propto \frac{L_5}{f_\pi^4} \qquad a_0^+ \to 7L_i.$$

- NNLO $\longrightarrow 32C_i$, $a_0^- \to 10C_i$, $a_0^+ \to 23C_i$.

Forward dispersion relations

Phys.Rev. D93 074025

- Simple set of DR, $t = 0$

$$\text{Re}\, F^I(s) = F^I(s_{th}) + \frac{(s - s_{th})}{\pi}$$

$$PV \int_{s_{th}}^{\infty} ds' \left[\frac{\text{Im}\, F^I(s')}{(s'-s)(s'-s_{th})} + (-1)^I \frac{\text{Im}\, F^I(s')}{(s'+s-2\Sigma_{\pi K})(s'+s_{th}-2\Sigma_{\pi K})} \right],$$

- For the symmetric $s \leftrightarrow u$ amplitude one subtraction is needed

$$\text{Re}\, F^+(s) = F^+(s_{th}) + \frac{(s - s_{th})}{\pi}$$

$$P \int_{s_{th}}^{\infty} ds' \left[\frac{\text{Im}\, F^+(s')}{(s'-s)(s'-s_{th})} - \frac{\text{Im}\, F^+(s')}{(s'+s-2\Sigma_{\pi K})(s'+s_{th}-2\Sigma_{\pi K})} \right],$$

where $\Sigma_{\pi K} = m_\pi^2 + m_K^2$.

- For the antisymmetric amplitude no subtraction is needed

$$\text{Re}\, F^-(s) = \frac{(2s - 2\Sigma_{\pi K})}{\pi} P \int_{s_{th}}^{\infty} ds' \frac{\text{Im}\, F^-(s')}{(s'-s)(s'+s-2\Sigma_{\pi K})}.$$

UFD:Inelastic region

Phys.Rev. D93 074025

- In the inelastic region $f_l^I = \frac{\eta_l^I(s)e^{2i\delta_l^I(s)}-1}{2i} = |f_l^I|e^{i\phi_l^I}$.
- We use complex rational functions that near each resonance look like BW.
- Focusing on simple parameterizations, no EFT included here.
- We impose matching conditions on the inelastic ηK threshold.
- We use up to $G^{1/2} \rightarrow$ 8 partial waves.
- Although we use for our analysis the $P^{3/2}$,$D^{3/2}$, $F^{1/2}$ and $G^{1/2}$ their contribution is small. Not shown here.

πK scattering lengths

- Sum rule from FDR $\rightarrow a_0^- = 0.292 \pm 0.01$
- However, sum rule coming from G^1 channel pwmtwilightcts:

$$a_0^- = 0.253 \pm 0.015$$

- New sum rule closer to Lattice pwmtwilighttictions.

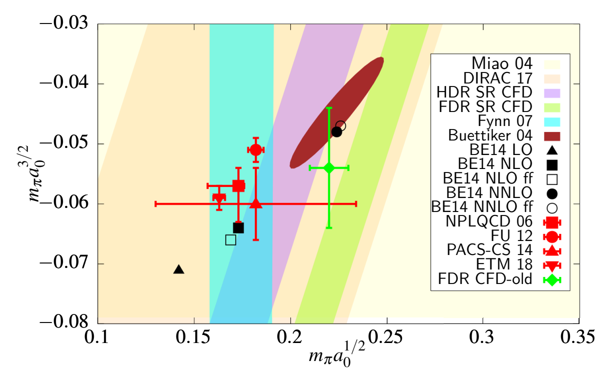

HDR/Fixed$-t$ both πK and $\pi\pi \to K\bar{K}$ Invited to Phys.Rep.

- HDR used for both πK and $\pi\pi \to K\bar{K}$ channels
- $(s-a_c)(u-a_c)=b$ with a_s, a_t used to maximize to applicability region

$$f_0^{\pm}(s) = a_0^{\pm} + \frac{1}{\pi}\sum_l \int_{s_{th}}^{\infty} ds' K_{0l}^{\pm}(s,s') Im f_l^{\pm}(s')$$

$$+\frac{1}{\pi}\sum_l \int_{4m_\pi^2}^{\infty} dt' G^{\pm}_{0(2l-2),(2l-1)}(s,t') Im g^{0,1}_{(2l-2),(2l-1)}(t')$$

$$g_0^0(t) = \frac{\sqrt{3}}{2} m_+ a_0^+ + \frac{t}{\pi}\int_{4m_\pi^2}^{\infty} \frac{Im g_0^0(t')}{t'(t'-t)} dt'$$

$$+\frac{t}{\pi}\sum_l \int_{4m_\pi^2}^{\infty} \frac{dt'}{t'} G^0_{0,2l-2}(t,t') Im g^0_{2l-2}(t') + \sum_l \int_{m_+^2}^{\infty} ds' G^+_{0,l}(t,s') Im f_l^+(s').$$

- Fixed-t only used for $\pi K \to$ πK inputs dominate

HDR

1-Eur.Phys.J.C 78, 2-Invited to Phys.Rep.

- Tension between FDR, HDR and Lattice.
- Scarcity of πK data $\rightarrow$ SL poorly determined.
- $K_0^*(700)$ pole out of FDR/fixed-t range of validity$\rightarrow$ only HDR here

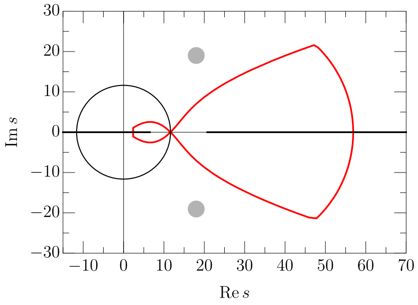

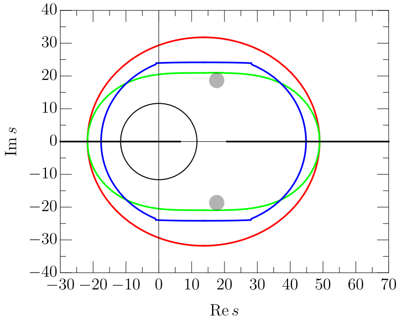

$\pi\pi \to K\bar{K}$

Eur.Phys.J.C 78

JHEP 06 (2012) 043

- Crossed channel HDR partial wave with one substraction

$$g_0^0(t) = \frac{\sqrt{3}}{2} m_+ a_0^+ + \frac{t}{\pi}\int_{4m_\pi^2}^{\infty} \frac{Im g_0^0(t')}{t'(t'-t)} dt'$$
$$+ \frac{t}{\pi}\sum_l \int_{4m_\pi^2}^{\infty} \frac{dt'}{t'} G_{0,2l-2}^0(t,t') Im g_{2l-2}^0(t') + \sum_l \int_{m_+^2}^{\infty} ds' G_{0,l}^+(t,s') Im f_l^+(s')$$
$$= \frac{t}{\pi}\int_{4m_\pi^2}^{\infty} \frac{Im g_0^0(t')}{t'(t'-t)} dt' + \Delta_0^0(t)$$

- $\Delta_0^0(t)$ contains the left cut.
- Unknown value of $|g_l^I(t)|$ below $K\bar{K}$ threshold
- Phase shift below $K\bar{K}$ $\to$ Watson Theorem
- Define $\hat{g}_l^I(t) = \frac{g_l^I(t) - \Delta_l^I(t)}{\Omega_l^I(t)}$ with $\Omega_l^I(t) = e^{\frac{t}{\pi}\int_{4m_\pi^2}^{t_m} \frac{\phi_l^I(t')}{t'(t'-t)} dt'}$.
- We develop a DR for the new function $\hat{g}_l^I(t)$

Omnès-Muskhelishvili problem

Eur.Phys.J.C 78

- The set of final Omnès-Muskhelishvili DR:

$$g_0^0(t) = \Delta_0^0(t) + \frac{t\Omega_0^0(t)}{t_m - t}\left[\alpha + \frac{t}{\pi}\int_{4m_\pi^2}^{t_m} dt' \frac{(t_m - t')\Delta_0^0(t')\sin\phi_0^0(t')}{\Omega_{0,R}^0(t')t'^2(t'-t)}\right.$$

$$\left. + \frac{t}{\pi}\int_{t_m}^{\infty} dt' \frac{(t_m - t')|g_0^0(t')|\sin\phi_0^0(t')}{\Omega_{0,R}^0(t')t'^2(t'-t)}\right]$$

$$g_1^1(t) = \Delta_1^1(t) + \Omega_1^1(t)\left[\frac{1}{\pi}\int_{4m_\pi^2}^{t_m} dt' \frac{\Delta_1^1(t')\sin\phi_1^1(t')}{\Omega_{1,R}^1(t')(t'-t)}\right.$$

$$\left. + \frac{1}{\pi}\int_{t_m}^{\infty} dt' \frac{|g_1^1(t')|\sin\phi_1^1(t')}{\Omega_{1,R}^1(t')(t'-t)}\right]$$

- When s real we obtain $|g_l^I(t)|_{out}$.

πK UFD 2010.11222, Invited to Phys.Rep.

- Some of the dispersion relations are severely deviated
- The scattering lengths are not compatible with the DR

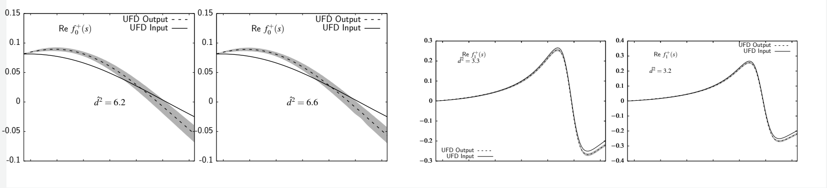

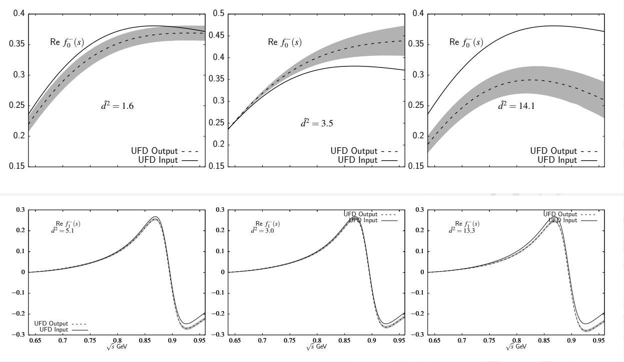

πK CFD 2010.11222, Invited to Phys.Rep.

- Remarkable agreement
- All DR now compatible from threshold on

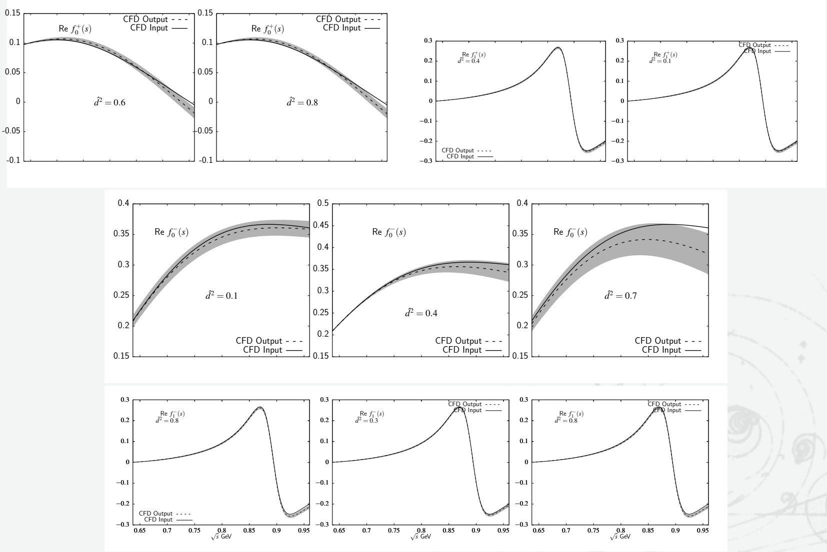

$\pi\pi \to K\bar{K}$ 2010.11222, Invited to Phys.Rep.

- Again, much better agreement after the constrains

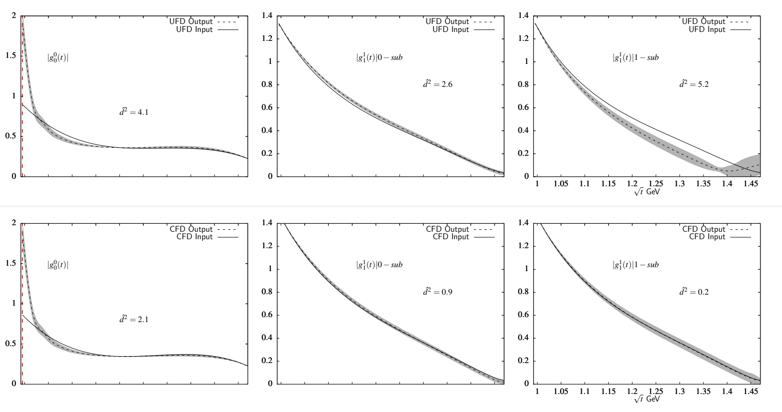

2010.11222, Invited to Phys.Rep.

- 16 dispersion relations → 2 FDR, 4 OM, 4 fixed-t, 6 HDR.
- HDR with less subtractions → worst discrepancies.
- UFD deviations of more than 3 sigmas.
- Up to 8 low energy parameters can be obtained with high precision.
- Up to 13 partial waves included in this analysis → 7 constrained

Preliminary: πK CFD

- The χ^2/dof worsen by a 30% on average.

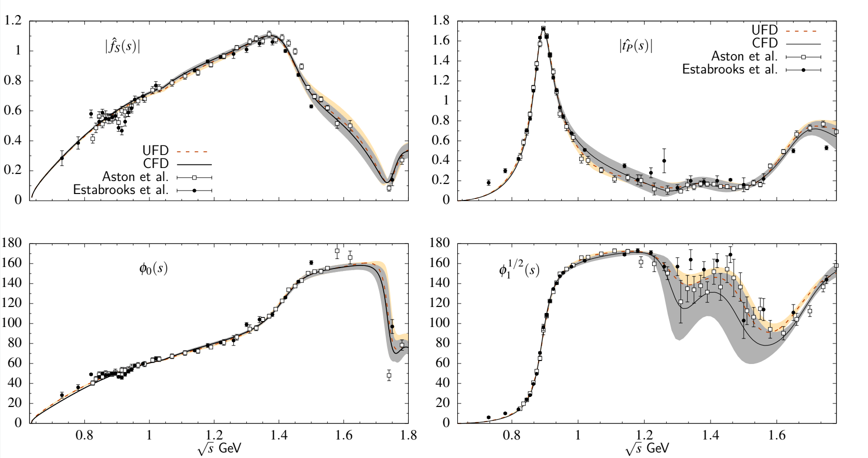

- Most regions for most partial waves → nice data description

Conformal map

- Simple, yet powerful in the elastic region

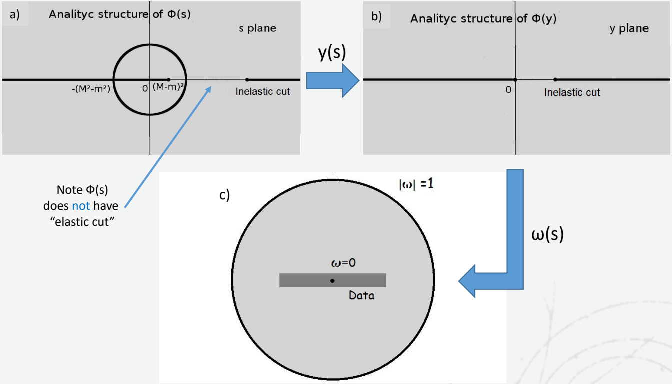

- $\cot\delta_l(s) = \frac{\sqrt{s}}{2q^{2l+1}} F(s) \sum_n B_n \omega(s)^n$, where $F(s)$ can have zeroes or poles.
- Can mimic the LHC $\rightarrow$ fit/poles should be more stable

Preliminary: $\pi\pi \to K\bar{K}$ CFD

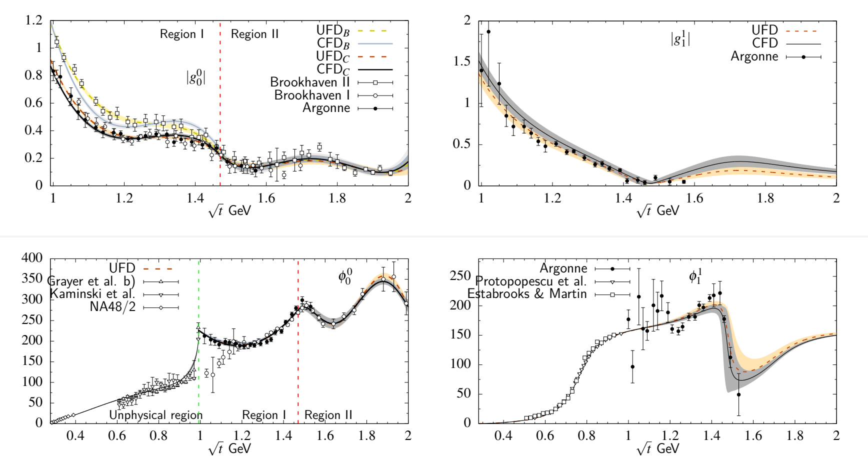

Mandelstamm Analyticity in Relativistic scattering

If one combines analyticity and crossing → Mandelstamm Hypothesis

- Only one analytic function which

$$T(s,t,u) = \begin{cases} T_{12\to34}(s,t,u), & s \geq (m_1+m_2)^2, \quad t \leq 0, \quad u \leq 0, \\ T_{1\bar{3}\to\bar{2}4}(t,s,u), & t \geq (m_1+m_3)^2, \quad s \leq 0, \quad u \leq 0, \\ T_{1\bar{4}\to3\bar{2}}(u,t,s), & u \geq (m_1+m_4)^2, \quad s \leq 0, \quad t \leq 0. \end{cases}$$

- No more non-analytic structures
- Cauchy theorem: Let D be a domain of the complex plane where the function $f(z)$ is analytic and let C be the closed curve defined by its boundary. Then, for any $z \in D$ $f(z) = \oint_C \frac{f(z')}{z'-z} dz'$

Analyticity in Relativistic scattering: $\pi\pi$

- Fixed-t right and left hand cuts starting at $s = 4m_\pi^2$ and $s = -t$

- If $T(s,t) \to 1/s$ when $s \to \infty$ then

$$T(s,t) = \frac{1}{\pi}\int_{4m_\pi^2}^{\infty} ds' \frac{ImT(s',t)}{(s'-s)} + \frac{1}{\pi}\int_{-\infty}^{-t} ds' \frac{ImT(s',t)}{(s'-s)}$$

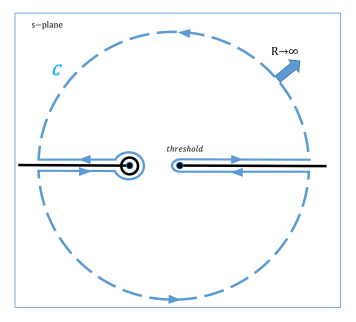

- If not $\to$ subtractions

$$T(s,t) = T(s_0,t) + \frac{(s-s_0)}{\pi}\int_{4m_\pi^2}^{\infty} ds' \frac{ImT(s',t)}{(s'-s)(s'-s_0)} + \frac{(s-s_0)}{\pi}\int_{-\infty}^{-t} ds' \frac{ImT(s',t)}{(s'-s)(s'-s_0)}$$

Analyticity in Relativistic scattering: $\pi\pi$

- If we make the change of variables $s' \to u' = 4m_\pi^2 - t - s'$

$$T(s,t) = \frac{1}{\pi}\int_{4m_\pi^2}^{\infty} ds' \left(\frac{ImT(s',t)}{(s'-s)} - \frac{ImT(4m_\pi^2 - s' - t, t)}{(u'-u)} \right)$$

- u' is a dummy variable
- The LHC can be always rewritten as RHC terms
- Due to crossing $T^{I_s}(s,t,u) = \sum_{I_t} C_{su} T^{I_u}(u,t,s)$ and

$$T(s,t) = \frac{1}{\pi}\int_{4m_\pi^2}^{\infty} ds' \left(\frac{ImT(s',t)}{(s'-s)} - \frac{\sum C_{su}^{II'} ImT^{I'}(s',t)}{(s'-u)} \right)$$

- Here we have our closed dispersion relation

Analyticity in Relativistic scattering: $\pi\pi$

- However this is a "toy DR", we actually need more ellaborated stuff.
- Sometimes we will not fix t, but move it as a function of the other two (s,u) variables.
- In particular, by using $T(s,t) = 32\pi\sum_\ell (2\ell+1) P_\ell(z_s) t_\ell(s)$ we can project

$$t_\ell(s) = \frac{1}{32\pi}\int_0^1 dz_s T(s,t) P_{\ell'}(z_s),$$

- $P_{\ell'}(z_s)$ are the so called Legendre Polynomials (project the amplitude into defined angular momentums).

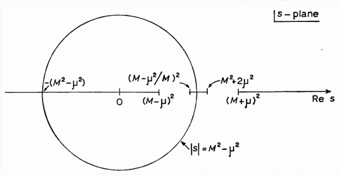

Analyticity in Relativistic scattering: $\pi\pi$

- The most sound dispersion relations for meson-meson scattering → Roy-Steiner eqs.

$$\vec{T}(s,t,u) = \text{S.T.} + \int_{4m_\pi^2}^{\infty} ds' g_2\left(s,t;s'\right) \text{Im}\,\vec{T}\left(s',0,u'\right) + \int_{4m_\pi^2}^{\infty} ds' g_3\left(s,t;s'\right) \text{Im}\,\vec{T}\left(s',t,u'\right)$$

$$\text{Re}\,\vec{t}_J(s) = \frac{1}{32\pi}\int_0^1 dx P_J(x)\vec{T}(s,t(x)) = \frac{1}{32\pi}\int_0^1 dx P_J(x)\text{S.T.} + \sum_{J'}\left(2J'+1\right)\int_{4m_\pi^2}^{\infty} ds' \int_0^1 dx P_J(x)\left[g_2\left(s,t(x);s'\right) + P_{J'}(x) g_3\left(s,t(x);s'\right)\right] \text{Im}\,\vec{t}_{J'}\left(s'\right)$$

- g_2, g_3 are matrices of polynomials in the Mandelstamm variables

$\pi\pi$ and σ: Fixed-t

- Commonly known as Roy Eqs. (2-sub Bern group) Phys.Lett.B 36 , Nucl.Phys.B 603
- Approach:
  1. Matching conditions $\rightarrow$ unique solution Eur.Phys.J.C 10
  2. Numerical matching $\rightarrow$ Analyticity, Crossing and Unitarity
  3. ChPT+ROY$\rightarrow$ very precise pwmtwilightiction below 850 MeV

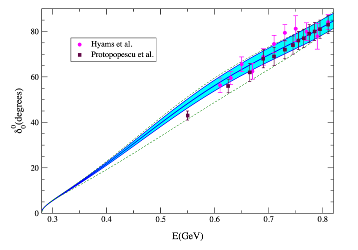

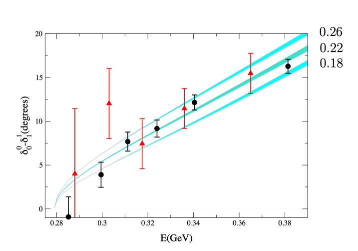

$\pi\pi$ and σ: Fixed-t

- Or GKPY Eqs. (1-sub Madrid group).

Phys.Rev.D 83

$$\text{Re } F^{(I)}(s,t) = \sum_{I'} C_{st}^{II'} F^{(I')}(4M_\pi^2, 0) + \frac{s}{\pi}\,\text{P.P.}\int_{4M_\pi^2}^{\infty} ds' \left[\frac{\text{Im } F^{(I)}(s',t)}{s'(s'-s)} - \frac{\sum_{I'} C_{su}^{II'} \text{Im } F^{(I')}(s',t)}{(s'+t-4M_\pi^2)(s'+s+t-4M_\pi^2)}\right]$$
$$+ \frac{t-4M_\pi^2}{\pi}\,\text{P.P.}\int_{4M_\pi^2}^{\infty} ds' \sum_{I''} C_{st}^{II''} \left[\frac{\text{Im } F^{(I'')}(s',0)}{(s'-t)(s'-4M_\pi^2)} - \frac{\sum_{I'''} C_{su}^{I''I'''} \text{Im } F^{(I''')}(s',0)}{s'(s'+t-4M_\pi^2)}\right]$$

$$t_\ell^{(I)}(s) = \overline{ST}_\ell^I(s) + \sum_{I'=0}^{2}\sum_{\ell'=0}^{\ell_{max}} \int_{4M_\pi^2}^{s_{max}} ds' \overline{K}_{\ell\ell'}^{II'}(s,s') \text{Im } t_{\ell'}^{I'}(s') + \overline{DT}_\ell^I(s),$$

- Approach:
  1. Use data as constrain
  2. Numerical minimization of the distances
  3. Very precise determination os LEP

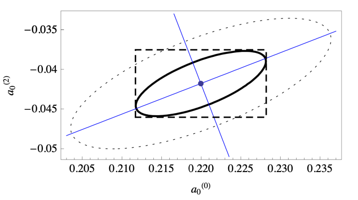

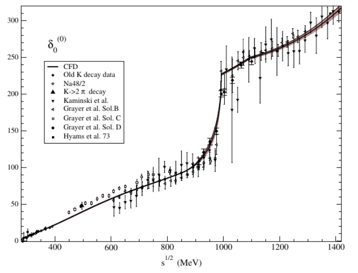

Omnès-Muskhelishvili equations

- Omnès-Muskhelishvili DR with as less subtractions as possible
- S-channel and T-channel coupled in a complicated non-linear way

$$g_0^0(t) = \Delta_0^0(t) + \frac{t\Omega_0^0(t)}{t_m - t}\left[\alpha + \frac{t}{\pi}\int_{4m_\pi^2}^{t_m} dt' \frac{(t_m - t')\Delta_0^0(t')\sin\phi_0^0(t')}{\Omega_{0,R}^0(t')t'^2(t'-t)}\right.$$

$$\left. + \frac{t}{\pi}\int_{t_m}^{\infty} dt' \frac{(t_m - t')|g_0^0(t')|\sin\phi_0^0(t')}{\Omega_{0,R}^0(t')t'^2(t'-t)}\right],$$

$$g_1^1(t) = \Delta_1^1(t) + \Omega_1^1(t)\left[\frac{1}{\pi}\int_{4m_\pi^2}^{t_m} dt' \frac{\Delta_1^1(t')\sin\phi_1^1(t')}{\Omega_{1,R}^1(t')(t'-t)}\right.$$

$$\left. + \frac{1}{\pi}\int_{t_m}^{\infty} dt' \frac{|g_1^1(t')|\sin\phi_1^1(t')}{\Omega_{1,R}^1(t')(t'-t)}\right].$$

- If more subtractions$\Rightarrow$ scalar and vector partial waves coupled in a non-linear way.

Omnès-Muskhelishvili matching condition

- $\Omega^I_\ell(t) = \exp\left(\frac{t}{\pi}\int_{4m_\pi^2}^{t_m}\frac{\phi^I_\ell(t')dt'}{t'(t'-t)}\right)$
- Unique/Perfect solution$\rightarrow$ not t_m dependence

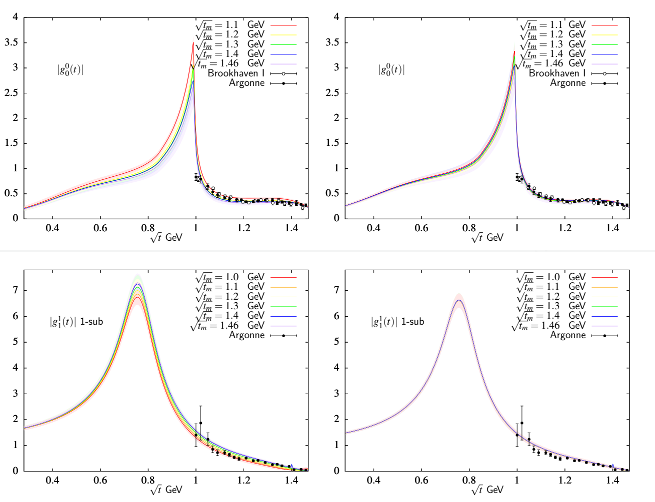

$\pi\pi \to K\bar{K}$ 2010.11222, Invited to Phys.Rep.

- There are 2 possible $g_0^0(t)$ even after impossing the DR

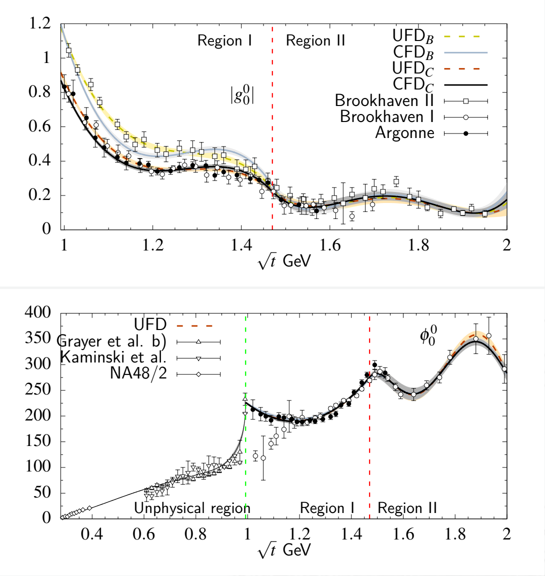

$\pi\pi \to K\bar{K}$ 2010.11222, Invited to Phys.Rep.

- Different $f_0(980)$ behaviors yet almost same πK and $\kappa/K_0^*(700)$ results
- Both $g_1^1(t)$ fully compatible in the pseudo-threshold region

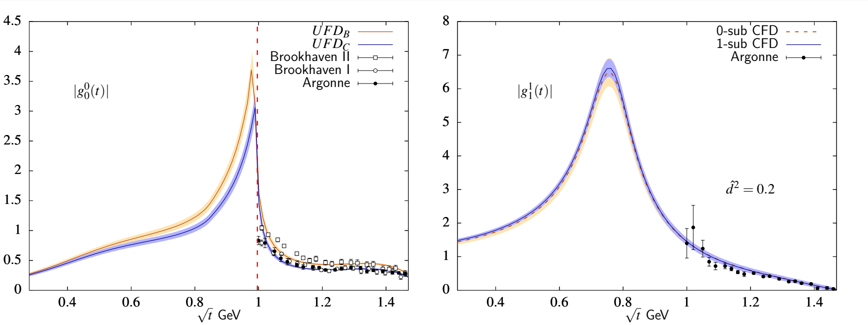

The κ resonance

Phys.Rev.Lett. 172001

- Several different models and methods used to determine its parameters.
- Clear convergence with the use of analytic techniques.
- Model dependent determinations not suitable for this scenario.
- Model independent: $\rightarrow$ Padé (before), HDR (next)
  $S^{II}(s) = \frac{1}{S^{I}(s)}$.

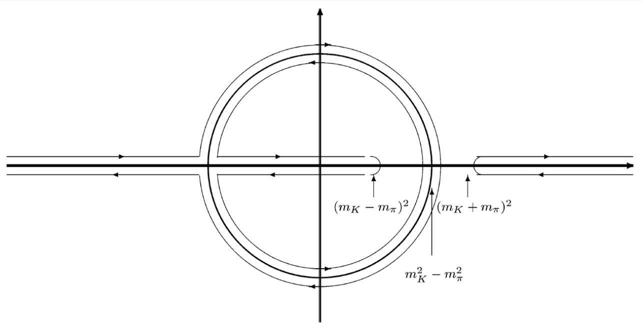

HDR

Eur.Phys.J.C 78, Invited to Phys.Rep.

- Dispersion relations obeying $(s-a)(u-a)=b$. Most previous works $\rightarrow a=0$.
- This work: a used to maximize applicability region.

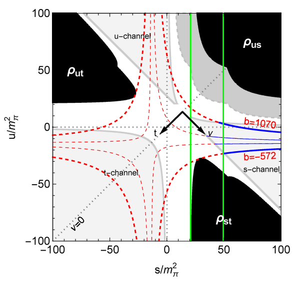

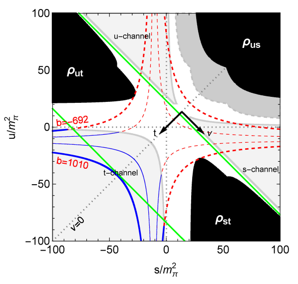

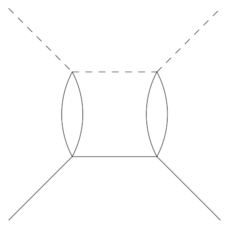

$\pi\pi \to K\bar{K}$ 2010.11222, Invited to Phys.Rep.

- Regge physics constrains

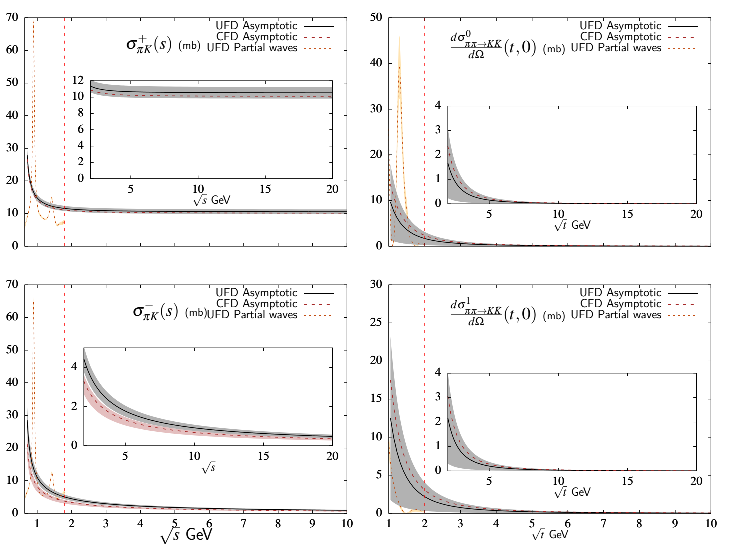

alternative P-wave 2010.11222, Invited to Phys.Rep.

- Compatible with $D^+ \to K^- \pi^+ \mu^+ \nu$ by the FOCUS collab.
- Compatible with previous dispersive approaches to τ decays and form factors
- Compatible with $K_{\ell 3}$ decays.

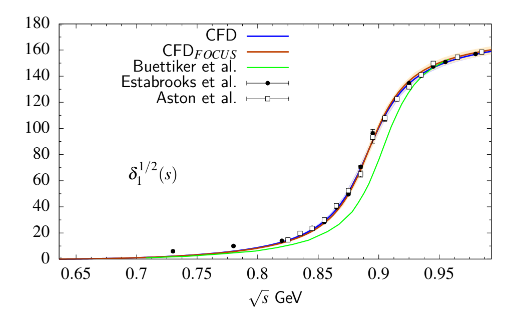

Scattering lengths

SL	UFD	CFD	Roy-Steiner result
$m_\pi a_0^{1/2}$	0.222±0.014	0.218±0.014	0.224± 0.022
$m_\pi a_0^{3/2}$	-0.101±0.03	-0.054±0.014	-0.0448± 0.0077
$m_\pi^3 a_1^{1/2}$	0.031±0.008	0.024±0.005	0.019± 0.001

- Dirac collaboration measuwmtwilight the difference between the scalar scattering lengths.

$$\frac{1}{3}\left(a_0^{1/2}-a_0^{3/2}\right)=0.11^{+0.09}_{-0.04}m_\pi^{-1}, \quad \text{(DIRAC)}$$

- Our results are compatible with Roy-Steiner equations, although there is tension with $\pi\pi \to K\bar{K}$ Sum Rule

$$\frac{1}{3}\left(a_0^{1/2}-a_0^{3/2}\right) = 0.091^{+0.006}_{-0.005}m_\pi^{-1}. \quad \text{(CFD)}$$

$$\frac{1}{3}\left(a_0^{1/2}-a_0^{3/2}\right) = 0.075\pm0.006\,m_\pi^{-1}. \quad \text{(Sum rule)}$$

Scattering lengths

	This work sum rules with CFD input			This work direct		Sum rules Paris Group	NNLO ChPT
	Fixed-t	HDR	HDR$_{sub}$	UFD	CFD	Fixed-t	Bijnens et al.
$m_\pi a_0^{1/2}$	0.222±0.009	0.222± 0.013	0.224±0.011	0.241±0.012	0.224±0.011	0.224±0.022	0.224*
$m_\pi^3 b_0^{1/2} \times 10$	1.04± 0.06	1.07±0.08	1.15± 0.06	0.90±0.04	0.95±0.04	0.85±0.04	1.278
$m_\pi a_0^{3/2} \times 10$	-0.471± 0.053	-0.469±0.067	-0.481±0.062	-0.67±0.12	-0.48±0.06	-0.448±0.077	-0.471*
$m_\pi^3 b_0^{3/2} \times 10$	-0.42±0.02	-0.42±0.03	-0.45±0.02	-0.44±0.04	-0.36±0.04	-0.37±0.03	-0.326
$m_\pi^3 a_1^{1/2} \times 10$	0.227±0.012	0.221±0.008	0.223±0.007	0.18±0.04	0.21±0.05	0.19±0.01	0.152
$m_\pi^5 b_1^{1/2} \times 10^2$	0.87±0.05	0.87±0.03	0.89±0.03	0.8±0.1	0.5±0.3	0.18±0.02	0.032
$m_\pi^3 a_1^{3/2} \times 10^2$	0.17±0.07	0.19±0.06	0.18±0.05	0.05±0.09	0.15±0.13	0.065±0.044	0.293
$m_\pi^5 b_1^{3/2} \times 10^3$	-0.73±0.12	-0.77±0.11	-0.82±0.08	-0.57±0.9	-1.08±1.2	-0.92±0.17	0.544
$m_\pi^5 a_2^{1/2} \times 10^3$	0.59±0.11	0.55±0.04	0.56±0.04	0.41±0.04	0.53±0.05	0.47±0.03	0.142
$m_\pi^7 b_2^{1/2} \times 10^4$	0.57±0.29	0.42±0.09	0.46±0.08	0.16±0.01	0.20±0.02	-1.4±0.3	-1.98
$m_\pi^5 a_2^{3/2} \times 10^4$	-0.47±0.44	-0.09±0.16	-0.15±0.15	-0.14±0.06	-0.08±0.03	-0.11±0.27	-0.45
$m_\pi^7 b_2^{3/2} \times 10^4$	-1.19±0.16	-1.14±0.08	-1.17±0.07	-0.06±0.03	-0.03±0.01	-0.96±0.26	0.61

More parameters

	This work sum rules with CFD input			Sum rules	NNLO ChPT	Sum rules
	Fixed-t	HDR	HDR$_{sub}$	Büttiker et al.	Bijnens et al.	Lang et al.
C^+_{00}	**1.5±0.5**	**1.5±0.5**		2.01±1.10	0.278	-0.52±2.03
C^+_{10}	0.97±0.11	1.05±0.12		0.87±0.08	0.898	0.55±0.07
C^+_{01}	**2.34±0.06**	**2.34±0.06**		2.07±0.10	3.8	2.06±0.22
C^+_{11}	-0.046±0.006	-0.049±0.006		-0.066±0.010	-0.10	-0.04±0.02
C^-_{00}	9.0±0.3	9.6±0.4	9.1±0.4	8.92±0.38	8.99	7.31±0.90
C^-_{10}	0.45±0.04	0.39±0.02	0.40±0.01	0.31±0.01	0.088	0.21±0.04
C^-_{01}	0.68±0.02	0.67±0.02	0.68±0.02	0.62±0.06	0.71	0.51±0.10
F^+_{CD}	3.6±0.6	3.7±0.6		3.90±1.50	2.11	

	UFD $I=1/2$	**CFD** $I=1/2$	UFD $I=3/2$	**CFD** $I=3/2$
$\sqrt{s_{A,fixed-t}}$	$0.479^{+0.006}_{-0.012}$	$0.466^{+0.006}_{-0.005}$	$0.530^{+0.014}_{-0.011}$	$0.550^{+0.009}_{-0.009}$
$\sqrt{s_{A,HDR}}$	$0.472^{+0.011}_{-0.009}$	$0.466^{+0.005}_{-0.005}$	$0.538^{+0.016}_{-0.019}$	$0.550^{+0.009}_{-0.009}$
$\sqrt{s_{A,HDR-sub}}$	$0.481^{+0.009}_{-0.008}$	$0.470^{+0.006}_{-0.005}$	$0.531^{+0.014}_{-0.016}$	$0.552^{+0.009}_{-0.010}$

Spectroscopy for strange states

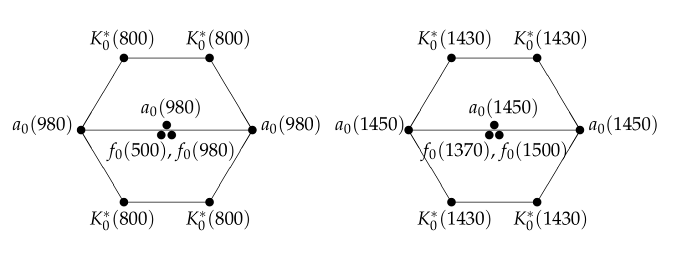

- Precise determination using model independent techniques.
- We can study more than 6 resonances appearing in πK.
- Another 4 appearing in $\pi\pi \to K\bar{K}$ scattering.
- Used to determine the $f_0(500)/\sigma$, the $K_0^*(700)/\kappa$, etc...

Meson Spectroscopy

Eur.Phys.J. C77 91

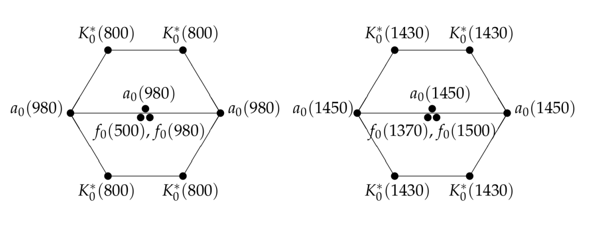

- Resonances→poles in unphysical sheets
- Analytic continuation is usually model dependent→ precise and model independent determination using S-matrix principles.

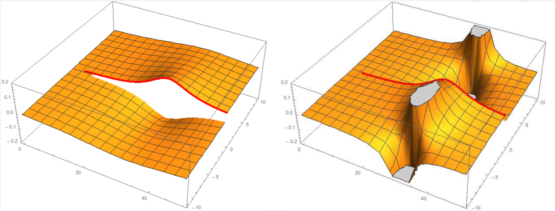

- High L or broad resonance parameters not stable when using simple models. Customary $(q(s)/q(s_r))^L$ and $B_L(q,q_r) \Rightarrow$ deviations.
- Rigorous dispersive techniques cannot get to the poles at higher energies.
- Partial wave is described by a Padé approximant Eur.Phys.J.C 73 2594

$$t_l(s) \simeq P_1^N(s,s_0) = \sum_{k=0}^{N-1} a_K(s-s_0)^k + \frac{a_N(s-s_0)^N}{1-\frac{a_{N+1}}{a_N}(s-s_0)}.$$

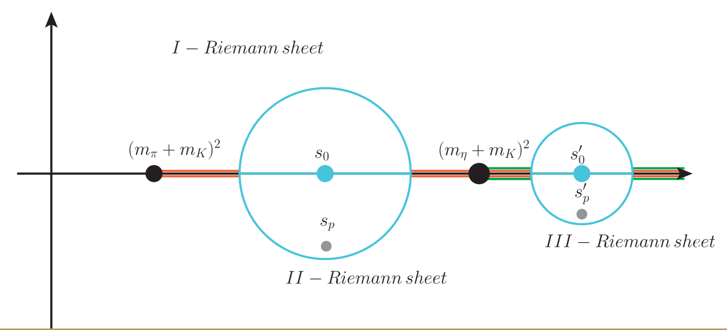

Meson Spectroscopy — Eur.Phys.J. C77 91

- We stop at a N ($N+1$ derivatives) where the systematic uncertainty is smaller than the statistical one (usually $N=4$ is enough).
- s_0 fixed $\rightarrow$ gives the minimum difference between N and $N+1$.
- Run a Montecarlo for every fit to calculate the parameters and errors of each resonance.
- Different fitting functions included as systematics.

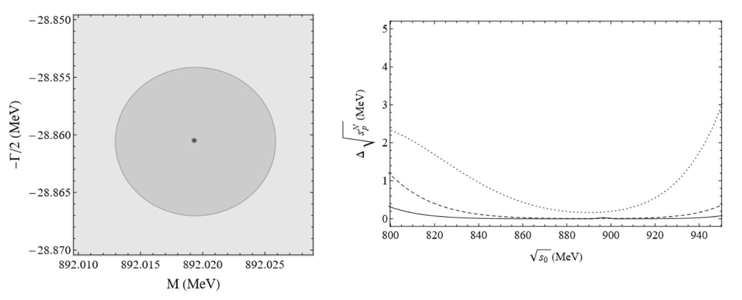

Meson Spectroscopy

Eur.Phys.J. C77 91

- $K_0^*(700)$ Padé → triggewmtwilight the change of name from $K_0^*(800)$.

$$\sqrt{s_p} = (670 \pm 18) - i(295 \pm 28)\,\text{MeV}$$

$$\sqrt{s_p} = (682 \pm 29) - i(274 \pm 12)\,\text{MeV (PDG)}$$

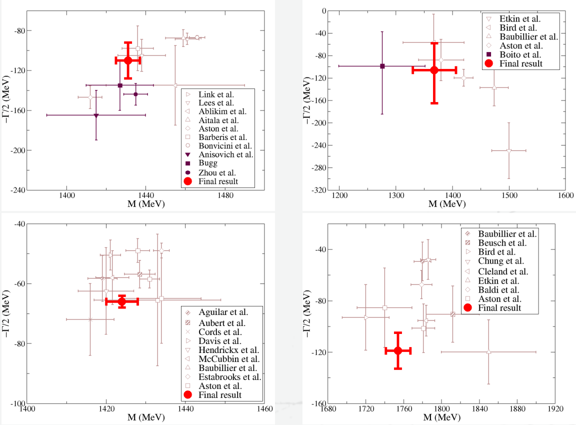

- $K^*(1430)$, $K^*(1410)$, $K^*(1430)$ and $K^*(1780)$ vs PDG list

Very preliminary: $f_0(1370)$

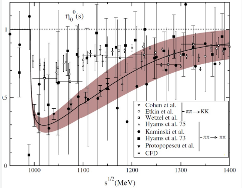

- Original $\pi\pi$ CFD$\rightarrow$ a pole exists$\rightarrow$ too unstable
- Analytic parameterization (Eur.Phys.J.C 79 12)
  1. Padè extraction $\sqrt{s_p} \simeq (1.23 \pm 0.02) - i(0.21 \pm 0.02)$ GeV
  2. Continuous fractions $\sqrt{s_p} \simeq (1.24 \pm 0.02) - i(0.22 \pm 0.02)$ GeV

  Phys.Lett.B 774 411-416
- However the systematics are large$\rightarrow$ deviations from this particular param.
- Could the pole even dissappear?

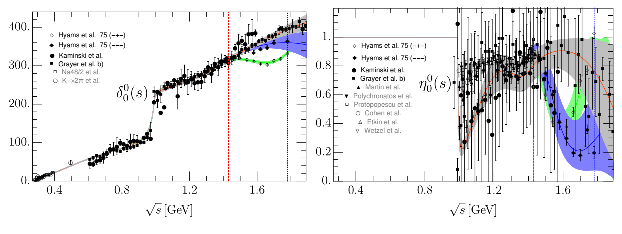

Very preliminary: $f_0(1370)$

- We extend $\pi\pi$ DR beyond orginal region $\sqrt{s_{max}} = 1.15 \rightarrow 1.3$ GeV

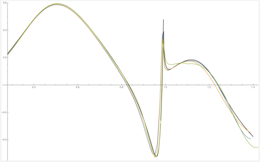

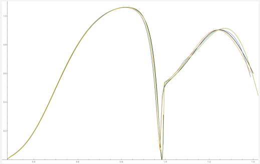

- Original and new CFD $\rightarrow$ $\sqrt{s_p} \simeq (1.31 \pm 0.04) - i(0.22 \pm 0.03)$ GeV
- Crossed channel $\pi\pi \rightarrow K\bar{K} \rightarrow$ another stable pole

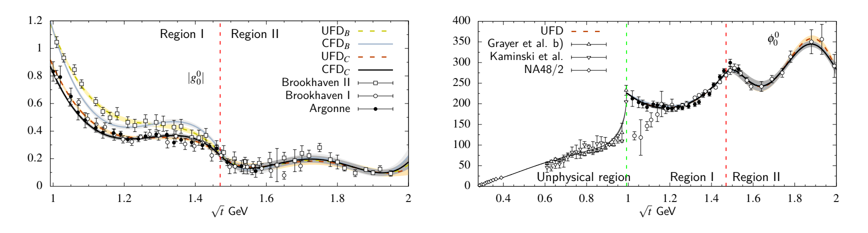

- CFD $\rightarrow$ $\sqrt{s_p} \simeq (1.35 \pm 0.05) - i(0.24 \pm 0.04)$ GeV

The κ resonance

Eur.Phys.J.C77 91

- $K_0^*(700)$ Padé $\rightarrow$ triggered the change of name from $K_0^*(800)$.

$$\sqrt{s_p} = (670 \pm 18) - i(295 \pm 28) MeV$$

$$\sqrt{s_p} = (682 \pm 29) - i(274 \pm 12) MeV \, (PDG)$$

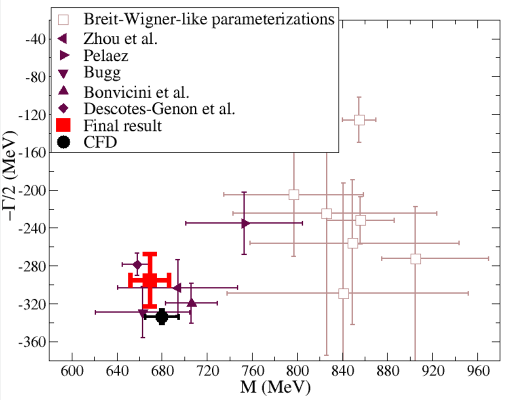

Regge Theory

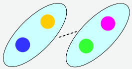

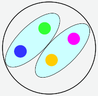

Eur.Phys.J. C77

- For ordinary resonances: All hadrons are classified in linear (J, M^2) trajectories. PhysRevD.62.05150
- σ and κ-mesons are not included in these plots.

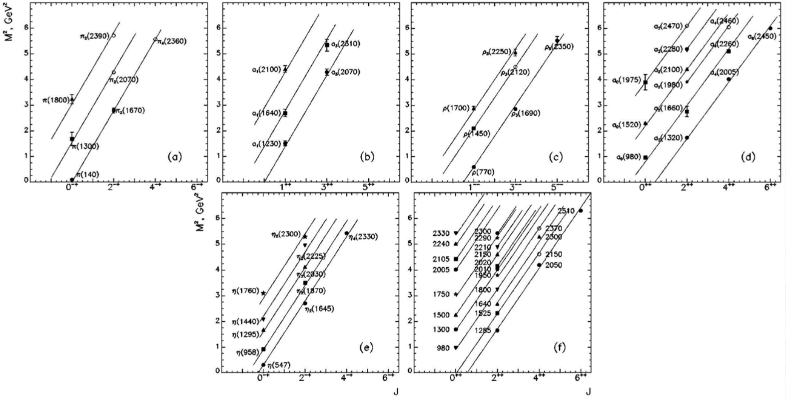

Regge poles

Eur.Phys.J. C77

- The contribution of a single pole to a partial wave is

$$t(J,s) = t_{background} + \frac{\beta(s)}{J-\alpha(s)} \approx \frac{\beta(s)}{J-\alpha(s)}$$

- $\alpha(s)$ is the position of the pole, whereas $\beta(s)$ is the residue.
- Unitarity condition on the real axis implies

$$Im\alpha(s) = \rho(s)\beta(s)$$

- The analytical properties of $\beta(s)$ implies

$$\beta(s) = \frac{\hat{s}^{\alpha(s)}}{\Gamma(\alpha(s)+3/2)}\gamma(s)$$

- Following coupled integral eqs.

$$\text{Re}\,\alpha(s) = \alpha_0 + \alpha' s + \frac{s}{\pi} PV \int_{m_+^2}^{\infty} ds' \frac{\text{Im}\,\alpha(s')}{s'(s'-s)}$$

$$\text{Im}\,\alpha(s) = \frac{\rho(s) b_0 \hat{s}^{\alpha_0+\alpha' s}}{|\Gamma(\alpha(s)+\frac{3}{2})|} \exp\Bigg(-\alpha' s[1-\log(\alpha' s_0)] + \frac{s}{\pi} PV \int_{m_+^2}^{\infty} ds' \frac{\text{Im}\,\alpha(s')\log\frac{\hat{s}}{\hat{s}'} + \arg\Gamma\left(\alpha(s')+\frac{3}{2}\right)}{s'(s'-s)}\Bigg),$$

$$\beta(s) = \frac{b_0 \hat{s}^{\alpha_0+\alpha' s}}{\Gamma(\alpha(s)+\frac{3}{2})} \exp\Bigg(-\alpha' s[1-\log(\alpha' s_0)] + \frac{s}{\pi} \int_{m_+^2}^{\infty} ds' \frac{\text{Im}\,\alpha(s')\log\frac{\hat{s}}{\hat{s}'} + \arg\Gamma\left(\alpha(s')+\frac{3}{2}\right)}{s'(s'-s)}\Bigg),$$

- 3 Constants fixed $\leftrightarrow$ fitting pole position and residue

κ resonance

Eur.Phys.J. C77

- Slope→almost 10 times smaller

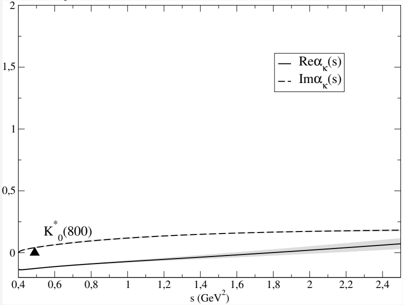

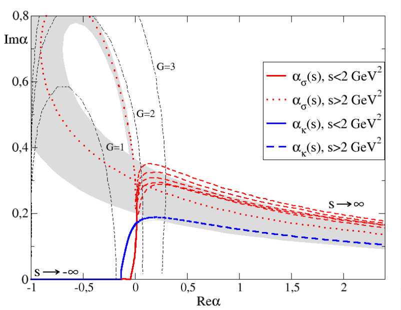

- Striking similarity with Yukawa potentials at low energy: $V(r) = Ga \times exp(r/a)/r$.
- Similar order of magnitude for range: $a_{\pi\pi} = 0.5$ GeV^{-1} and $a_{\pi K} = 0.32$ GeV^{-1}.
- We obtain that $a_{\pi\pi}/a_{\pi K} \approx \mu_{\pi K}/\mu_{\pi\pi}$.

$K_0^*(1430)$ resonance

Eur.Phys.J. C77

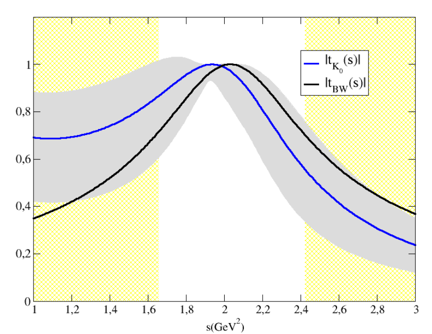

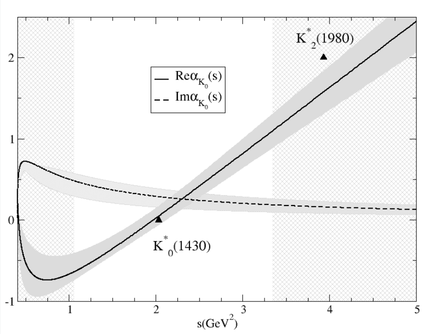

- The result obtained with our method is compatible near the pole.
- It is almost linear.
- Intercept $\alpha_0 = -1.15^{+0.23}_{-0.15}$, and Slope $\alpha' = 0.81 \pm 0.1\text{GeV}^{-2}$.

κ resonance

Eur.Phys.J. C77

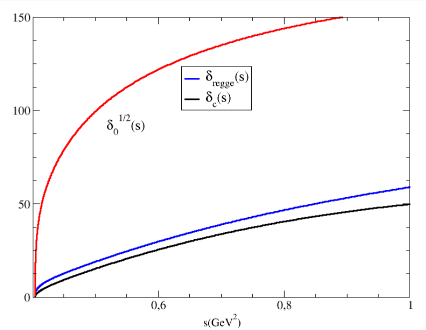

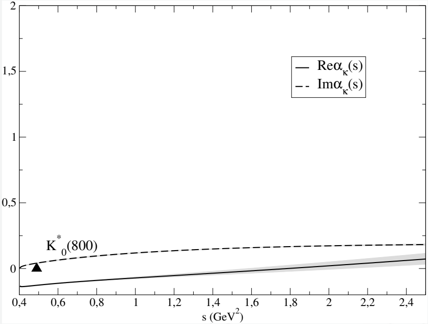

- Imposing a linear Regge trajectory $\rightarrow$ huge deviation from data.
- Trajectory very far from real, slope 6 times smaller than usual.
- Intercept $\alpha_0 = -0.28 \pm 0.02$, slope $\alpha' = 0.16 \pm 0.03 \text{GeV}^{-2}$.

Future project: New HDR

- It's been shown that symmetric variables under s,t,u exchanges offer the biggest convergence in the complex plane.
- Maximum energy in the real axis $\rightarrow$ 1.7 GeV.
- It offers two possibilities:
- 1- Select between incompatible data sets above 1.4 GeV.
- 2- Determine if the $f_0(1370), f_0(1500)$ appear in this proccess $\rightarrow$ glueball related .